


Structure and mechanical behavior of lignosulfonate-treated piassava (*Attalea funifera*) fibers

Paula Lage Agrize¹, Beatriz Dantas Lourenço da Silva¹, Betina Carvalho Veiga¹, Camila Aparecida Abelha Rocha¹, Fabio da Costa Garcia Filho², Fábio de Oliveira Braga¹ 

¹Universidade Federal Fluminense, Departamento de Engenharia Civil. Rua Passo da Pátria 156, São Domingos, 24210-240, Niterói, RJ, Brasil.

²Instituto Militar de Engenharia, Seção de Engenharia de Materiais. Praça General Tibúrcio 80, Praia Vermelha, 22290-270, Rio de Janeiro, RJ, Brasil.

e-mail: paula.agrize@gmail.com, beatrizdantas@id.uff.br, betinaveiga@id.uff.br, camilaabelha@id.uff.br, fabiogarciafilho@ime.eb.br, fabiobraga@id.uff.br

ABSTRACT

The use of natural lignocellulosic fiber (NLF) biocomposites for the construction industry has been growing over the years, due to technical and environmental advantages. However, fiber-matrix incompatibility remains a major challenge. Various surface treatments have been investigated to improve fiber-matrix bonding, including sodium lignosulfonate (SLS), a potentially effective and environmentally friendly chemical. In this study, SLS treatment protocols were applied to piassava fibers to evaluate their influence on the fibers. Thermogravimetric Analysis (TG/DTG), X-ray Diffraction (XRD), Scanning Electron Microscopy (SEM/EDS), Fourier-transform Infrared Spectroscopy (FTIR), moisture absorption measurements and tensile tests were performed to characterize the modifications. Results demonstrated, for the first time, the efficiency of SLS to remove extractives from the piassava surface. In general, partial degradation of the cellulosic structure was observed, noticeable by the slight drop in crystallinity index (from 42.80 to 39.82%), and an increase in the TG residual mass (from 21.35 to 31.90%), along with changes in DTG curves. However, a particular SLS treatment using ultrasonic bath was able to fully clean the surface preserving the cellulosic structure, and increasing the strength of fibers (from 386 ± 140 MPa to 524 ± 126 MPa).

Keywords: Natural lignocellulosic fiber; Microstructure; Mechanical behavior; Surface treatment.

1. INTRODUCTION

Over the past few decades, increasing concern about the scarcity of natural resources and the generation of high volumes of waste in the construction industry has been leading to a preference for renewable materials and energy, as well as better waste destination and management [1]. According to the Brazilian Association of Public Cleaning and Special Waste (ABRELPE) [2], the civil construction industry is responsible for about 60% of the solid waste generated in Brazilian urban areas. In this scenario, the use of renewable natural lignocellulosic fibers (NLF) as biocomposite reinforcement for building materials has been growing over the years [3–10].

NLFs display several advantages that enable them to be used in biocomposites such as high specific strength and Young's modulus, as well as good thermal insulation, low cost of production, biodegradability, and low abrasiveness. NLFs as reinforcements are considered more sustainable when compared to manufactured fibers, as their production/processing consumes less fossil fuel, reduces carbon footprint by absorbing CO₂ during plant growth, as well as recovers energy by end-of-life incineration [11].

The piassava fiber is a promising NLF for civil construction applications. Piassava is the common designation for the fibers obtained from the *Attalea funifera* palm tree. It is a long, strong, stiff, and almost impermeable NLF, of wide availability in the market. It is mostly available in the northeastern region of Brazil, in states such as Bahia, Alagoas, and Sergipe. Each *Attalea funifera* tree can provide around 8 to 10 kg of piassava fibers per year [12]. Currently, most of the Brazilian piassava fiber is used to produce brooms and brushes. Due to their good technical properties, several researchers have been investigating piassava fibers for biocomposites [13–19].

MONTEIRO *et al.* [10] performed a comprehensive review of the properties of NLFs for biocomposites. For the piassava fibers, they reported values of tensile strength in the wide range of 109 to 1750 MPa,

as well as density varying from 1.0 to 1.4 g/cm³ and Young's Modulus from 6 to 7 GPa. MIRANDA *et al.* [18] performed a physicochemical characterization of the piassava fibers subjected to several chemical treatments. They found that the piassava fibers are mainly composed of cellulose (~52%), hemicellulose (~3.5%), and lignin (~43%) [18]. REBELO *et al.* [16] found that the crystallinity index of piassava was around 60%. They reported [16] also two main thermal decomposition events in a temperature program for the piassava fibers: the first occurs at around 250 °C, attributed to hemicellulose decomposition, while the second, attributed to cellulose decomposition, occurs at temperatures around 350 °C. The authors also note that the decomposition of lignin can vary depending on the NLF species and occurs within a temperature range from 150 to 450 °C [16].

Despite all the advantages of the NLFs, their hydrophilic nature is one of the main drawbacks for a wider application. This tends to impair the fiber-matrix bonding in such biocomposites. In particular, for composites produced using cementitious materials as matrix, NLFs may present in its composition substances that may affect the hydration of the cement, affecting also the curing process. Aiming to avoid that, surface pretreatments are usually performed prior to incorporation into the matrix to enhance interfacial adhesion and to reduce the effects on biocomposite durability [15–19]. Alkaline treatments, for example, are efficient to remove amorphous extractives from plant fibers, increasing the crystallinity index and resistance to thermal degradation, and improving the fiber-matrix adhesion. Some of the recently investigated pretreatments on piassava fibers are graphene oxide-coating [15], mercerization with NaOH [16, 17] and Ca(OH)₂ [17], acid treatment with H₂SO₄ [18], and acetylation [18].

One promising treatment that has recently been considered is the fiber modification with lignosulfonates (LSs) [20–24]. LSs are lignin derivatives (biomass), by-products of the sulfite pulping of wood in the papermaking industry. According to RUWOLDT [25], LSs are commonly used as dispersants, as in concrete plasticizers, drilling mud thinners, and dye dispersants. Their molecular structure provides amphiphilic properties and thus can link to several surfaces and interfaces. These applications suggest that LSs treatment might be promising surface modifiers for NLFs to improve the fiber-matrix bonding, especially in cementitious composites [20–22]. GUALBERTO *et al.* [22] investigated the effects of modifying sisal fibers with sodium LS (SLS) for use in cementitious composites. The authors found that the SLS treatment reduced fiber moisture absorption and improved composite durability. OLIVEIRA *et al.* [21] studied the modification of sisal fibers with SLS, however, composites with phenolic and LS-based matrices were produced, with good results. LI *et al.* [23] were able to modify the hydrophilic nature of cellulose fibers into hydrophobic by introducing layers of cationic polyacrylamide and LS into to the fibers surface. Higher hydrophobicity was observed when the LS was the outermost layer [23]. While SLS treatments have had good results in treating sisal and cellulose fibers, there has been no investigation focusing on the response of piassava fibers to these treatments.

In this context, the present work investigates, for the first time, the physicochemical modifications that the LS treatment causes in piassava (*Attalea funifera*) fibers in terms of microstructure, water absorption and mechanical behavior.

2. MATERIALS AND METHODS

2.1. Materials

The piassava (*Attalea funifera*) fibers used in this study were donated by Vassouras Rossi Ltda., a broom manufacturer located in Petropolis (Rio de Janeiro/Brazil). The fibers were received as a burden weighting approximately 2 kg. Thicker fibers (which were more defective) were disregarded, while thinner fibers with diameters ranging from 200 to 600 µm were selected for the study. An example of the fiber, as observed under an optical microscope, is shown in Figure 1.

Sodium lignosulfonate (SLS) was used to prepare the solutions for the surface treatment of the piassava fibers. The SLS was type 1259 Ultrazine NA (CAS No. 8061-51-6), donated by *Lignotec Brasil* (Brazil), a company from the Borregaard Lignotec Group. According to the manufacturer, Ultrazine NA is based on highly refined and modified SLS derived from spruce wood and sulfite liquor. It was provided as a brown water-soluble powder. Table 1 shows some basic specifications of the chemical.

2.2. Methods

The fibers were categorized into four different groups: three groups underwent SLS treatment protocols, while the remaining group served as the control group and was not subjected to SLS treatment. The fibers from the control group, called “Raw Piassava”, were soaked in deionized water for 1 hour at 70 °C. After each treatment, the fibers were dried at 104 ± 2 °C until constant mass was achieved.

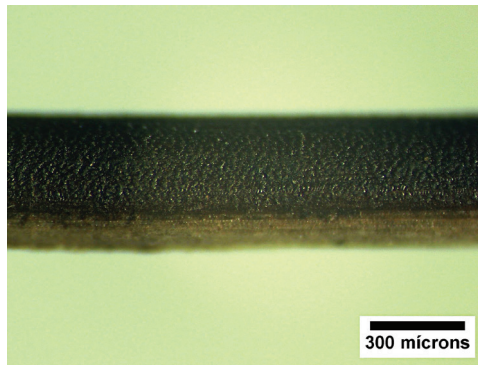


Figure 1: Optical micrograph of the piassava surface, obtained in a model LAB-60T Laborana stereomicroscope. Magnification: $\sim 60\times$.

Table 1: Sodium lignosulfonate (SLS) specifications.

LIGNOSULFONATE SPECIFICATIONS	
pH (10% solution)	8.7 ± 0.8
Insolubles (w/w)%	Max. 0.1
Sodium (%)	7
Calcium (%)	Max. 0.1
Chloride (%)	Max. 0.10
Alkali (%)	Max. 12
Reducing sugars (%)	1

Table 2: SLS treatments and specimen designation.

TREATMENT PROTOCOL	SPECIMEN DESIGNATION
1h immersion in water at 70 °C	Raw piassava
1 h immersion in 5 wt.% SLS solution at 70 °C	PL-70-1h
24 h immersion in 5 wt.% SLS solution at 25 °C	PL-24h
1 h immersion in 5 wt.% SLS solution at 25 °C with ultrasonic irradiation	PL-1h-US

To carry out the SLS treatment protocols, a 5 wt.% SLS solution in deionized water was used. These specific protocols were selected based on their positive outcomes for another NLF, namely the sisal fiber [21]. They are detailed in Table 2.

Ultrasonic irradiation was produced in a laboratory ultrasonic bath (model SoniClean 2PS from Sanders) at a frequency of 40 kHz. The aim of using the ultrasonic energy was to enhance the surface free energy of the fibers and activate the surface to accept the SLS molecules. The ultrasonic vibration is known to cause cavitation, a phenomenon of formation and outbreak of bubbles [21].

To determine the statistical distributions of piassava fiber diameters, fibers were measured using an Olympus BX3M optical microscope. The fibers were placed on a cardboard fillet in the microscope holder and examined at $10\times$ magnification. A total of 40 fibers from each treatment were observed and measured. X-ray diffraction (XRD) test was conducted to assess the changes in fiber crystallinity resulting from the several treatment protocols. The XRD analyzes were performed in a model D8 Advance Polycrystal Bruker diffractometer. Measurements were performed using Cu-K α radiation, within the 2θ range of 10° to 70° , with a scanning velocity of $2^\circ/\text{min}$ and a step size of 0.05° . This particular 2θ range was chosen to encompass the diffraction peaks of the crystalline cellulose [26, 27]. For sample preparation, the fibers were cut to lengths of less than 1 mm.

To calculate the Crystallinity Index (X_c) of the piassava fibers, the diffraction patterns were analyzed using Origin 8 software to obtain data on the peaks of native cellulose (JCPDS data 03-0289) and amorphous phases. The X_c is calculated from Equation 1 [26, 27]:

$$X_c = \frac{I_{002} - I_{am}}{I_{002}} \cdot 100\% \quad (1)$$

Where: X_c is the crystallinity index; I_{002} is the maximum intensity of the (002) crystalline plane of the cellulose (2θ around 22°); I_{am} is the intensity of the minimum (2θ around 18°) between the peaks related to (002) and (101) planes of the cellulose ($2\theta \sim 22^\circ$ and $\sim 16^\circ$, respectively).

The fibers were analyzed by means of Fourier-Transform Infrared Spectroscopy (FTIR), in Attenuated Total Reflection (ATR) mode. The objective was to evaluate the chemical bond changes resulting from the several treatment protocols. As sample preparation, the fibers were ground in a cutting mill resulting in fine grains. The spectra were obtained using a model Spectrum 100 Perkin Elmer infrared spectrometer, in the range of $4000\text{--}650\text{ cm}^{-1}$. The resulting spectra were analyzed in accordance with the ASTM E2224 standard [28].

Thermogravimetric analysis (TGA) aimed to evaluate the thermal stability of the fibers. The tests were carried out in a model DTG-60 Shimadzu calorimeter, from 21 to $500\text{ }^\circ\text{C}$, at a heating rate of $10\text{ }^\circ\text{C}/\text{min}$, in a nitrogen atmosphere [15, 21]. The resulting spectra were analyzed in accordance with the ASTM E2550 standard [29].

Tensile tests were performed to analyze the mechanical behavior of the fibers. The tests were carried out in accordance with the ASTM C1557 standard [30], in a model Tytron 250 MTS testing machine. Ten specimens were tested for each treatment, with a test speed of $0.5\text{ mm}/\text{min}$, using a 5 kN load cell and a gauge length of 40 mm [30]. The experimental setup for the tensile test is shown in Figure 2.

The surface modifications of the fibers were evaluated using scanning electron microscopy (SEM). The SEM analyzes were performed in a model Quanta FEG 250 FEI equipment, with secondary electrons contrast to observe the surface morphology. The chemical composition of the fibers was determined by Energy-dispersive X-Ray spectroscopy (EDS) analysis, which allowed the images to be correlated to their chemical composition.

The moisture absorption capability of the fibers was evaluated by following the procedures outlined in ASTM E1756 [31] and E104 standards [32]. Samples of 500 mg were taken from each fiber condition and dried at $105 \pm 3\text{ }^\circ\text{C}$ for 24 h in previously dried aluminum weighting pans. The specimens were allowed to cool in a desiccator with silica gel, and their dry mass (m_d) was measured using an analytical balance with a precision of 0.1 mg . Next, the specimens were placed in a desiccator with a fixed relative humidity of 75% [22, 32] and their weight was measured after 1 h , 2 h , and 24 h . The moisture absorption ($\%Ab$) was calculated using Equation 2, as following:

$$\%Ab = \frac{m_{ft} - m_d}{m_d} \cdot 100\% \quad (2)$$

Where: $\%Ab$ is the moisture absorption (%); m_{ft} is the weight (g) for a particular exposure time in 75% relative humidity; m_d is the dry mass.

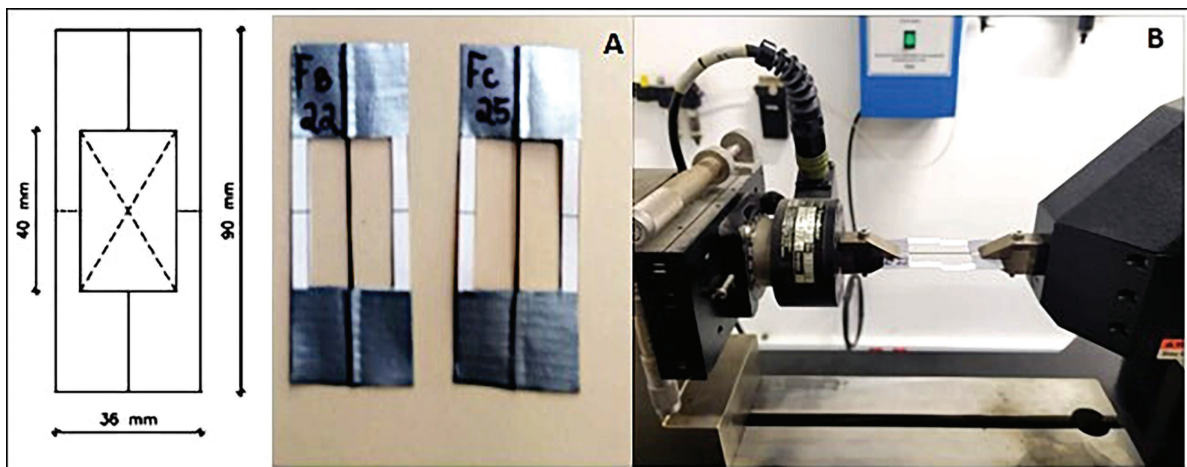


Figure 2: Tensile tests: (a) Schematic of the tabs and samples prepared for the tests; (b) Test execution.

3. RESULTS AND DISCUSSION

3.1. Diameter distribution

The statistical distribution of fiber diameters is shown in the histograms in Figure 3. Table 3 presents the maximum (D_{MAX}) and minimum (D_{MIN}) diameters found, along with the calculated average diameter (D_M) and standard deviation (σ).

The average values and distributions shown in Figure 3 and Table 3 are very similar, indicating that the starting points for diameter measurements are coincident for all treatment protocols. Given that SLS solution, in general, only provide a thin layer of crystallization products on the surface of fibers [21, 22], it was not expected that there would be any significant variation in diameter.

3.2. X-Ray Diffraction (XRD)

Figure 4 shows the diffraction patterns obtained for the piassava fibers. It shows that both Raw Piassava and the treated fibers (PL-70-1h, PL-24h and PL-1h-US) present diffraction peaks in the same angular positions, which demonstrates their cellulosic nature. Peaks related to the crystalline “native cellulose” phase (JCPDS data

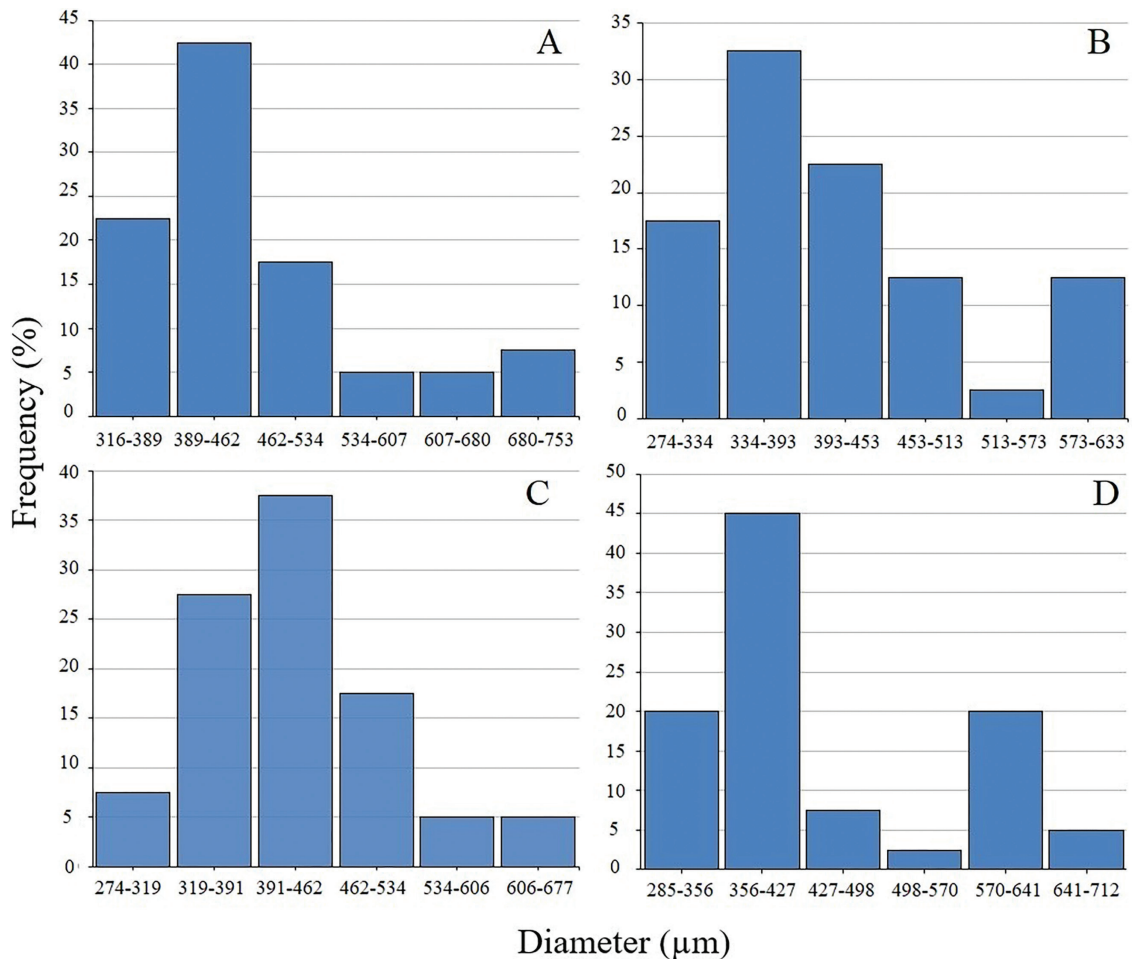


Figure 3: Diameter distributions for the fibers: (a) Raw Piassava; (b) PL-70-1h; (c) PL-24h; (d) PL-1h-US.

Table 3: Fiber diameter data.

SPECIMEN	D_{MAX} (mm)	D_{MIN} (mm)	D_M (mm)	σ (mm)
Raw Piassava	753	316	463	104
PL-70-1h	633	274	412	95
PL-24h	677	247	432	90
PL-1h-US	712	285	440	119

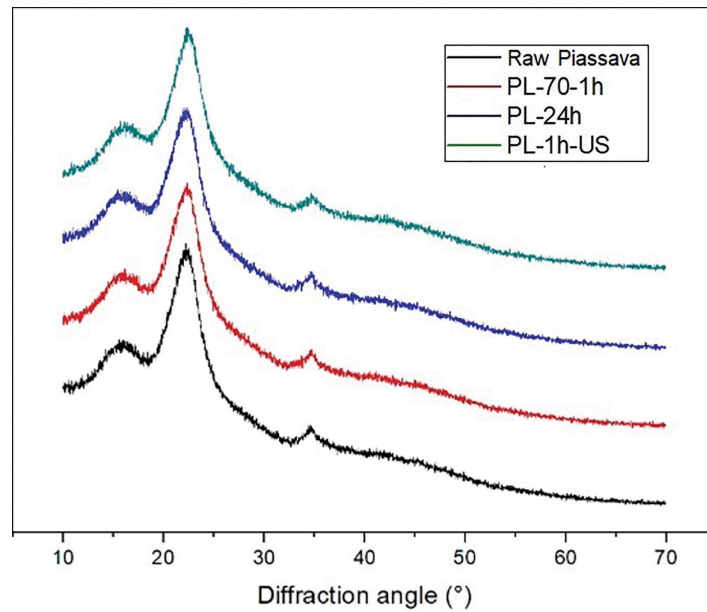


Figure 4: Diffraction (XRD) patterns for piassava fibers.

Table 4: Peak information from the XRD spectra of the raw and treated piassava fibers.

PEAK POSITION (DEGREES)	STRUCTURE	CRYSTALLINE PLANE
16	Cellulose I	(1 $\bar{1}$ 0) [35, 36]
22	Cellulose I	(200) [35, 36]
36	Cellulose I	(004) [35, 36]

Table 5: Peak intensity data and calculated crystallinity index (%CI) for the raw and treated fibers.

SPECIMEN	I_{002}	I_{am}	X_c (%)
Raw piassava	5517.965	3156.268	42.80
PL-70-1h	5174.405	3069.004	40.69
PL-24h	5143.455	3095.515	39.82
PL-1h-US	5181.658	2982.124	42.45
Average:			41.4 ± 1.4

03-0289) have been identified, as summarized in Table 4. Lignin and hemicellulose, however, are amorphous constituents [33, 34] and contribute to lower the crystallinity index.

Based on the diffraction patterns (Figure 4), and using Equation 1, the values of the crystallinity index (X_c) were calculated and are shown in Table 5. The calculated X_c values for all specimens were around 40% (Table 5), which are consistent with the values found on the literature [17, 18]. SANTOS *et al.* [14] obtained $X_c = 30\%$ for raw piassava fibers and $X_c = 44\%$ for mercerized fibers (using a 2% NaOH solution). REBELO *et al.* [16] obtained $X_c = 19\%$ for the raw piassava and $X_c = 30\%$ for mercerized piassava fibers. MIRANDA *et al.* [18] obtained higher values than the present work, $X_c = 62\%$ for raw piassava and $X_c = 65\%$ for mercerized fibers (using 10% NaOH solution). The increasing X_c values for mercerized fibers are expected since the treatment removes part of the lignin and hemicellulose. The differences found between values from literature [14, 16–18] and the ones from the present work might be attributed to the natural inhomogeneities of the fibers, due to differences in growth conditions and processing characteristics. In addition, PARK *et al.* [26] have identified some limitations of the peak height technique which could also contribute to the variation among the research groups [14, 16–18]: Natural misalignment in the apex of the amorphous halo relative to the minimum position between the (002) and the (101) peaks; Consideration of just one cellulose crystalline peak (002), not

considering the others; Not considering the peak width (crystallite size). Those assumptions are inherent to the peak height technique, dependent on the instrumentation and data processing (e.g. whether or not removing the diffraction pattern background). Therefore, PARK *et al.* [26] recommend that the peak height technique should be primarily used to compare relative differences in samples, such as the ones from the present work.

According to Table 5, the specimens PL-70-1h and PL-24h had a slight decrease in the X_c compared to the raw piassava. This might be caused by a decomposition phenomenon on the crystalline cellulose structure (since cellulose is the only relevant crystalline compound) [14]. This indicates, also, that PL-70-1h and PL-24h treatment protocols might not be as effective to remove amorphous compounds from the surface of the piassava fibers when compared to the treatment with only hot water (Raw Piassava). These phenomena, however, were less intense for the PL-1h-US specimen, which presented virtually the same value of X_c as the raw piassava.

3.3. Fourier Transform Infrared Spectroscopy (FTIR)

Figure 5 shows the FTIR spectra of the fibers. The spectra can be divided into two main wave number (WN) groups: a high WN range from 3750 to 2800 cm^{-1} , then a second region with lower WN, from 1800 to 650 cm^{-1} [14]. Typical bands from organic and lignocellulosic groups are present: 3340 cm^{-1} , attributed to OH stretching vibrations due to intramolecular hydrogen bonds [14, 18, 19]; 2920 and 2851 cm^{-1} from stretching of aliphatic C-H bonds (methyl and methylene groups) [14]; 1718 and 1238 cm^{-1} from C = O stretching vibration in acetyl and ester groups in lignin, hemicellulose and pectin [14, 18, 19, 35]; 1164 and 1032 cm^{-1} (C-O-C pyranose) [35] from stretching vibrations of C-O-C groups, present in glucose rings in cellulose and other compounds [14]; 898 cm^{-1} from β -glycosidic bonds in cellulose; 1607 (C = C), 1512 (C-H) [18] and 1421 (methoxyl, -O-CH₃) cm^{-1} , characteristic vibrations referring to lignin [36].

Analyzing the spectra in Figure 5, the main differences are related to band intensities. No absence of group bands could be noticed. Compared to the raw piassava spectrum, PL-70-1h and PL-24h spectra show less intense bands. Otherwise, PL-1h-US shows much higher intense bands. It is a generalized phenomenon since all bands in the spectrum are involved. In a recent paper, JOSE *et al.* [20] evaluated the modification of wool fabrics with the SLS solution, and they observed a similar phenomenon of generalized band shrinkage. They attributed the phenomenon to the successful modification of SLS to the wool fabric. Besides that, the presence of the same bands in all the spectra might be attributed to a low influence of the treatment in the bulk of piassava fibers.

3.4. Thermogravimetric Analysis (TGA)

Figure 6 exhibits the thermogravimetry (TG) curves for the fibers, while Figure 7 shows the differential thermogravimetry (DTG) curves. All curves in Figure 6 displays three specific features: (a) small weight drop (around 10%) below 100 °C due to the vaporization of moisture; (b) an intense weight loss (around 50%) in the 250–350 °C

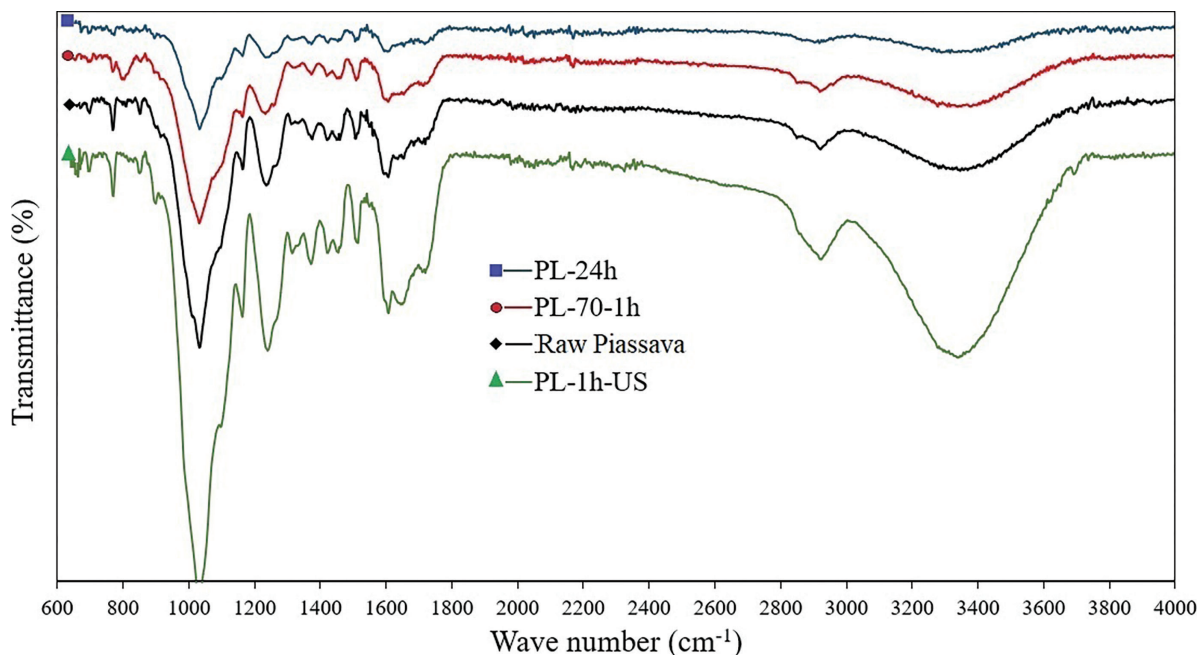


Figure 5: FTIR spectra for the raw and treated fibers.

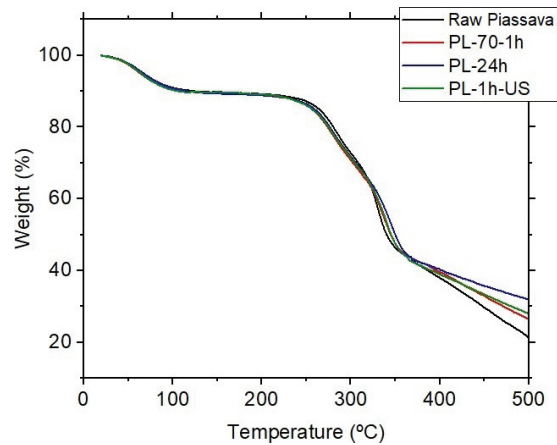


Figure 6: TG curves for the raw and treated fibers.

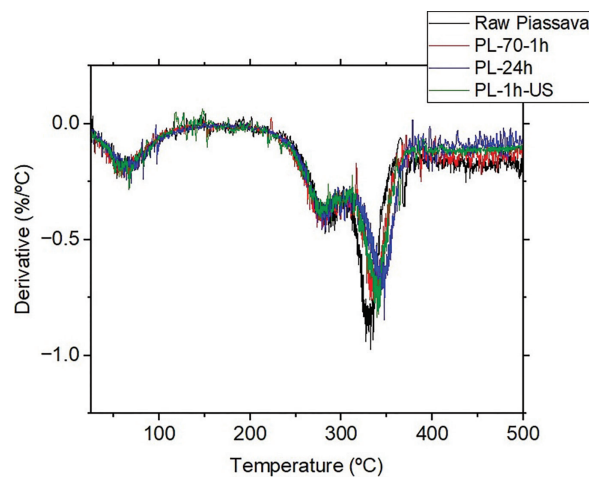


Figure 7: DTG curves for the raw and treated fibers.

range; (c) A smoother weight loss from 350 °C to 500 °C. It is well-known [18–21, 35–37] that (b) is caused by degradation and pyrolysis of hemicellulose (around 250 °C) and cellulose (around 350 °C). Regarding lignin, literature states it is the most difficult component to decompose [18, 37]. This reaction occurs very slowly, in a large range of temperatures (160–900 °C), so that the mass loss occurs in a very low rate [16, 18, 37], which could be imperceptible in the TG and DTG curves. Another important feature in Figure 6 is the differences in the residual mass (PL-24h > PL-1hUS > PL70-1h > Raw piassava). This might be attributed to the removal of organic components during the treatment, often related to hemicellulose/lignin/extractives removal, which might be considered beneficial, or cellulose degradation, which is not desirable. If the relation to the XRD results (Table 5) is considered, it would imply that PL-1h-US is losing mostly amorphous components (not cellulose) while PL-70-1h and PL-24h are losing a mix of cellulose and other amorphous components.

The changes in the different treatment protocols are highlighted in the DTG curves (Figure 7). All curves are identical until the temperature of cellulose decomposition around 350 °C. Beyond this point, the DTG peaks in the curves of the SLS-treated specimens (PL-70-1h, PL-24h, PL-1h-US) are shifted to higher temperatures and present a smaller internal area. This suggests that although some cellulose decomposition occurred (as evidenced by the drop in the crystallinity index, X_c), the remaining cellulose is less susceptible to further decomposition [21].

3.5. Tensile tests

Figure 8 depicts the tensile stress-strain curves for both untreated and treated piassava fibers, and Table 6 provides a summary of the results, including the strength (σ_u) and maximum deformation prior to fracture (ϵ_u). As shown in Figure 8, all specimens exhibit similar stress-strain behaviors, with an initial elastic response at

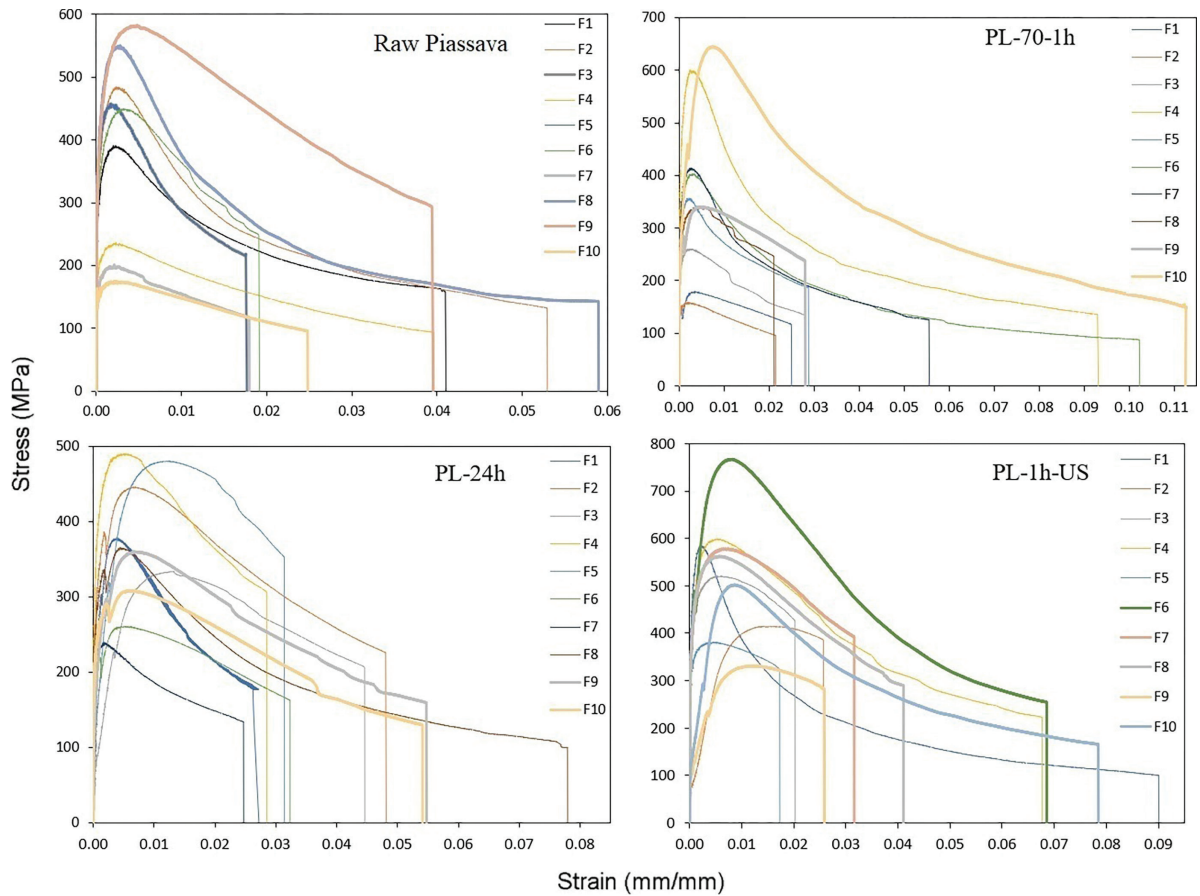


Figure 8: Tensile stress-strain curves for the raw and treated fibers.

Table 6: Tensile test data obtained from the stress-strain curves.

SPECIMEN	PROPERTY	SAMPLE										AVERAGE
		1	2	3	4	5	6	7	8	9	10	
Raw Piassava	σ_u (MPa)	357	236	457	390	484	450	201	550	558	175	386 ± 140
	ϵ_u (adm)	0.048	0.040	0.018	0.041	0.053	0.019	0.018	0.059	0.040	0.025	0.036 ± 0.015
PL-70-1h	σ_u (MPa)	179	158	260	600	356	403	414	338	340	644	369 ± 159
	ϵ_u (adm)	0.025	0.021	0.028	0.093	0.029	0.102	0.056	0.021	0.028	0.113	0.052 ± 0.037
PL-24h	σ_u (MPa)	377	446	333	490	480	261	239	365	360	308	366 ± 86
	ϵ_u (adm)	0.027	0.048	0.045	0.029	0.031	0.032	0.025	0.078	0.055	0.054	0.042 ± 0.017
PL-1h-US	σ_u (MPa)	584	414	520	598	381	767	578	562	331	502	524 ± 126
	ϵ_u (adm)	0.090	0.026	0.020	0.068	0.017	0.069	0.032	0.041	0.026	0.078	0.047 ± 0.027

low deformation values, followed by a large non-linear region until fracture. The results show broadly disperse numerical values for σ_u and ϵ_u (Table 6), which might be attributed to natural inhomogeneities of the fibers, such as variation in diameter and presence/absence of defects, as observed elsewhere [10].

PL-1h-US exhibited the highest strength values (524 ± 126 MPa) among all specimens. An analysis of variance (ANOVA) performed on the data confirmed a significant difference (p -value = 0.029542) between the strength averages, with 95% confidence. A Tukey's honest significant test (HSD) applied to the data showed that the significant difference is between PL-1h-US and PL-24h (p -value = 0.04884). The superiority of the PL-1h-US is consistent with the other results which indicated that the treatment preserves the cellulose structure while removing the impurities from the fibers.

The strength values obtained in this study for piassava fibers are within the range reported by MONTEIRO *et al.* [10]. More recent works, such as those by MIRANDA *et al.* [18] and D'ALMEIDA *et al.* [19], reported values closer to the bottom limit of the range reviewed by MONTEIRO *et al.* [10] and lower than those obtained in this study. In contrast, the ϵ_u values, did not show significant differences between specimens.

3.6. Scanning Electron Microscopy (SEM)

Figures 9 to 12 depict scanning electron micrographs of piassava fibers, revealing different surface morphologies resulting from different treatments. The raw piassava fibers (Figure 9) display a rough surface with impurities (extractives) present, while typical protrusions on piassava surface reported by other authors [10, 38] are not visible. EDS analysis indicated the presence of carbon (C), oxygen (O), calcium (Ca) and silicon (Si) on the surface. For PL-70-1h and PL-24h specimens (Figures 10 and 11, respectively), cleaner surfaces with the expected protrusions are visible, indicating removal of extractives. However, some impurities are still observed, albeit in a smoother morphology due to deposition of SLS crystals. EDS analysis showed the presence of C, O, Ca, Si, and sodium (Na) in PL-24h (Figure 10), and sulfur (S) in PL-70-1h (Figure 11), consistent with SLS absorption. Notably, the longer treatment (PL-24h) may cause damage to the fibers, evident by the extraction of natural protrusions and small cracks on the surface.

The PL-1h-US specimen exhibits a remarkably clean surface with well-defined protrusions and surface details, as evident from Figure 12. The treatment appears to be effective in removing the extractives without any fiber degradation, as all the protrusions are preserved, and no cracks are observed. The EDS analysis reveals no traces of SLS, with neither Na nor S detected indicating that PL-1h-US treatment is a reliable and effective method for extractive removal while maintaining the integrity of piassava fibers.

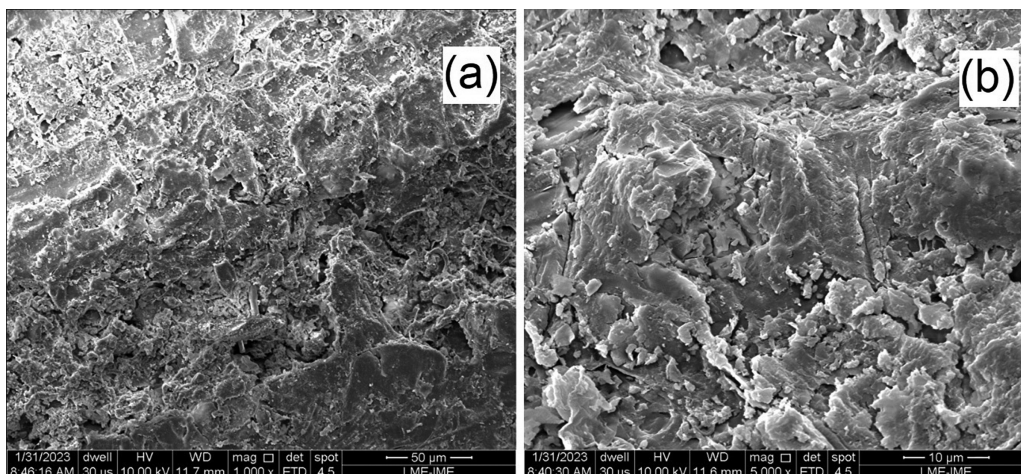


Figure 9: SEM micrographs for the Raw piassava fiber: (a) 1,000×; (b) 5,000×.

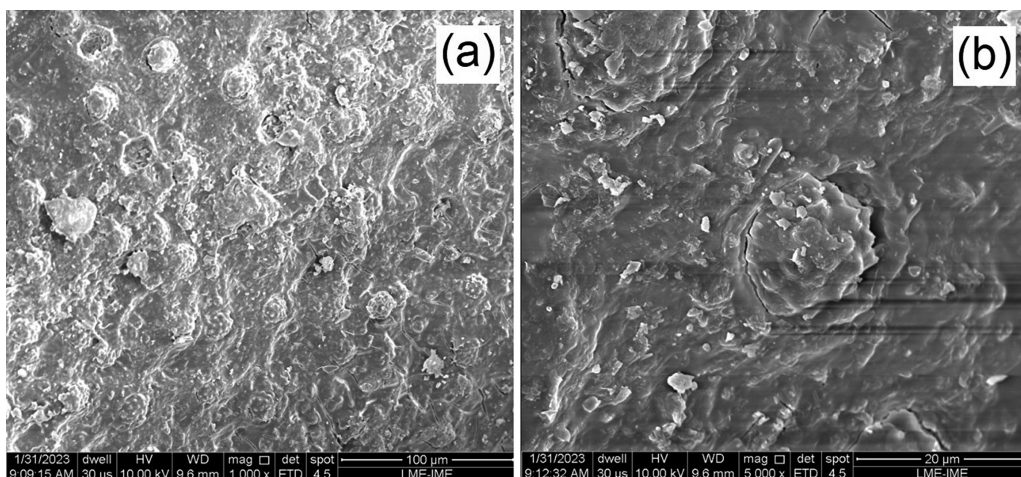


Figure 10: SEM micrographs for the PL-70-1h fiber: (a) 1,000×; (b) 5,000×.

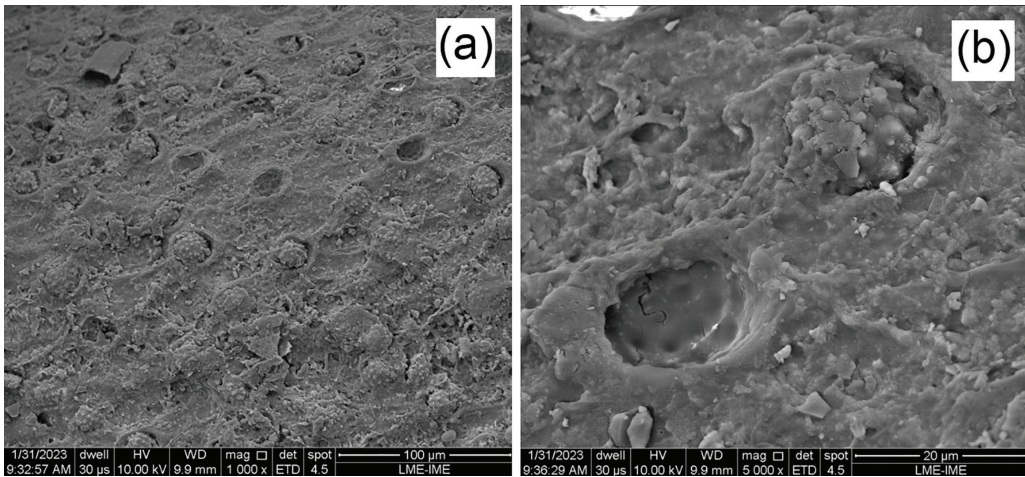


Figure 11: SEM micrographs for the PL-24h fiber: (a) 1,000×; (b) 5,000×.

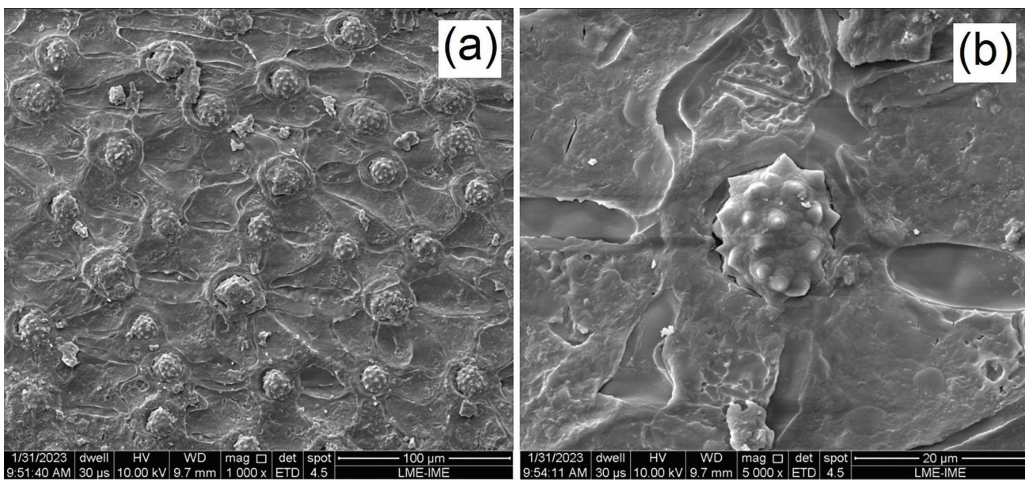


Figure 12: SEM micrographs for the PL-1h-US fiber: (a) 1,000×; (b) 5,000×.

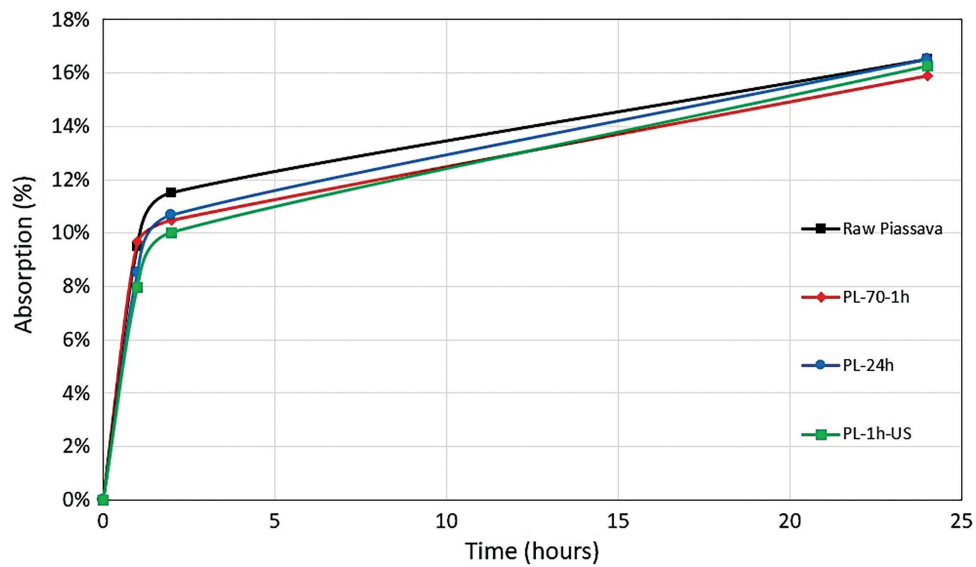


Figure 13: Moisture absorption of the fibers.

3.7. Moisture absorption

The moisture absorption of the fibers was depicted as a function of time in Figure 13. A tendency of reduced moisture absorption in the first hours after drying was observed in the SLS-treated fibers (PL-70-1h, PL-24h, and PL-1h-US). However, after 24 hours, the tendency was no longer observed, and the absorbed moisture of the SLS-treated fibers was virtually the same as that of raw piassava. The initial reduced moisture absorption may be attributed to the removal of hemicellulose due to SLS treatment since hemicellulose has the highest moisture absorption capacity [39]. The moisture absorption levels of approximately 15% in 24 hours were found to be consistent with the values of weight loss observed in the TG curve (Figure 6).

4. CONCLUSIONS

In the present work, several treatment protocols with sodium lignosulfonate (SLS) were applied to piassava fibers to evaluate the influence on the microstructure and mechanical behavior of the fibers. The treatment protocols included: (1) Raw Piassava (control group): 1-hour immersion in deionized water at 70 °C; (2) PL-70-1h: 1-hour immersion in 5 wt.% SLS solution at 70 °C; (3) PL-24h: 24-hour immersion in 5 wt.% SLS solution at room temperature (25 °C); (4) PL-1h-US: 1-hour immersion in 5 wt.% SLS solution in conjunction with ultrasonic irradiation (40 kHz). The main conclusions are presented below:

- The piassava fibers are partially crystalline, exhibiting the crystalline structure identified as native cellulose (JCPDS data 03-0289). PL-70-1h and PL-24h specimens presented smaller crystallinity indexes (40.69 and 39.82%, respectively), compared to the Raw piassava (42.80%), which is explained by partial degradation of the cellulosic structure. However, the PL-1h-US specimen presented near the same crystallinity index (42.45%) as Raw piassava, indicating preservation of the cellulosic structure.
- The thermogravimetric analysis (TGA) provided signs of removal of organic components during the treatment, related to hemicellulose/lignin/extractives removal. The differential thermogravimetric (DTG) curves show that (post-treatment) remaining cellulose is less susceptible to decomposition.
- The PL-70-1h and PL-24h treatment protocols were able to partially clean the piassava surface, exposing the fiber natural protrusions, but inducing SLS crystal deposits on the surface. The treatment for PL-1h-US, however, was able to produce very clean surfaces, exposing small surface details and protrusions in the fibers, also preserving the cellulosic structure.
- PL-1h-US was the treatment protocol in the present work with the best average strength values, reaching 524 ± 126 MPa. This indicates that the treatment preserves the cellulosic structure while removing the impurities from the fibers.
- A tendency of reduced moisture absorption in the first hours after drying was observed in the SLS-treated fibers, attributed to the removal of hemicellulose due to SLS treatment.

5. ACKNOWLEDGMENTS

The authors of the present work would like to thank: FAPERJ for funding the project in the Basic Research Aid (APQ1) Program, process 211.544/2021; UFF/Brazil Research Funding Program (FOPESQ 2021), for funding the project; Numats/UFRJ/Brazil for performing the tensile tests; LDRX/UFF for performing the XRD tests; Chemical Engineering Post-Graduation Program (SE/5) from IME/Brazil for performing the FTIR analyzes; RECAT/UFF/Brazil for performing the TGA; Lignotec Brasil, for the donation of the sodium lignosulfonate; Vassouras Rossi Ltda., for the donation of the piassava fibers.

6. BIBLIOGRAPHY

- [1] PURCHASE, C.K., AL ZULAYQ, D.M., O'BRIEN, B.T., *et al.*, "Circular economy of construction and demolition waste: a literature review on lessons, challenges, and benefits", *Materials (Basel)*, v. 15, n. 1, pp. 76–100, 2021. doi: <http://dx.doi.org/10.3390/ma15010076>. PubMed PMID: 35009222.
- [2] BRAZILIAN ASSOCIATION OF PUBLIC CLEANING AND SPECIAL WASTE COMPANIES, *Overview of the solid waste in Brazil*, ABRELPE, São Paulo, 2021. (in Portuguese)
- [3] ABEDI, M., HASSANSHAHI, O., RASHIDDEL, A., *et al.*, "A sustainable cementitious composite reinforced with natural fibers: an experimental and numerical study", *Construction & Building Materials*, v. 378, pp. 131093, 2023. doi: <http://dx.doi.org/10.1016/j.conbuildmat.2023.131093>
- [4] AHMAD, J., ARBILI, M.M., MAJDI, A., *et al.*, "Performance of concrete reinforced with jute fibers (natural fibers): a review", *Journal of Engineered Fibers and Fabrics*, v. 17, pp. 17, 2022. doi: <http://dx.doi.org/10.1177/15589250221121871>

- [5] SEKI, Y., SELLI, F., ERDOGAN, Ü.H., *et al.*, “A review on alternative raw materials for sustainable production: novel plant fibers”, *Cellulose (London, England)*, v. 29, n. 9, pp. 4877–4918, 2022. doi: <http://dx.doi.org/10.1007/s10570-022-04597-4>
- [6] JESUDASS, A., GAYATHRI, V., GEETHAN, R., *et al.*, “Earthen blocks with natural fibres – a review”, *Materials Today: Proceedings*, v. 45, n. 7, pp. 6979–6986, 2021. doi: <http://dx.doi.org/10.1016/j.matpr.2021.01.434>
- [7] AZEVEDO, A.R.G., LIMA, T.E.S., REIS, R.H.M., *et al.*, “Guaruman fiber: a promising reinforcement for cement-based mortars”, *Case Studies in Construction Materials*, v. 16, pp. e01029, 2022. doi: <http://dx.doi.org/10.1016/j.cscm.2022.e01029>
- [8] RIOFRIO, A., CORNEJO, M., BAYKARA, H., “Environmental performance of bamboo fibers and sugarcane bagasse reinforced metakaolin-based geopolymers”, *Case Studies in Construction Materials*, v. 17, pp. e01150, 2022. doi: <http://dx.doi.org/10.1016/j.cscm.2022.e01150>
- [9] SILVA, G., KIM, S., BERTOLOTTI, B., *et al.*, “Optimization of a reinforced geopolymer composite using natural fibers and construction wastes”, *Construction & Building Materials*, v. 258, pp. 119697, 2020. doi: <http://dx.doi.org/10.1016/j.conbuildmat.2020.119697>
- [10] MONTEIRO, S.N., LOPES, F.P.D., BARBOSA, A.P., *et al.*, “Natural lignocellulosic fibers as Engineering Materials - an overview”, *Metallurgical and Materials Transactions. A, Physical Metallurgy and Materials Science*, v. 42A, n. 10, pp. 2963–2974, 2011. doi: <http://dx.doi.org/10.1007/s11661-011-0789-6>
- [11] JOSHI, S.V., DRZAL, L.T., MOHANTY, A.K., *et al.*, “Are natural fiber composites environmentally superior to glass fiber reinforced composites?”, *Composites. Part A, Applied Science and Manufacturing*, v. 35, n. 3, pp. 371–376, 2004. doi: <http://dx.doi.org/10.1016/j.compositesa.2003.09.016>
- [12] BRAZILIAN INSTITUTE OF GEOGRAPHY AND STATISTICS. *Production of vegetal extraction and forestry*, Rio de Janeiro, IBGE, 2007. (in Portuguese)
- [13] NUNES, S.G., SILVA, L.V., AMICO, S.C., *et al.*, “Study of composites produced with recovered polypropylene and piassava fiber”, *Materials Research*, v. 20, n. 1, pp. 144–150, 2017. doi: <http://dx.doi.org/10.1590/1980-5373-mr-2016-0659>
- [14] SANTOS, F.M.R., SOUZA, T.F., BARQUETE, D.M., *et al.*, “Comparative analysis of the sisal and piassava fibers as reinforcements in lightweight cementitious composites with EVA waste”, *Construction & Building Materials*, v. 128, pp. 315–323, 2016. <http://dx.doi.org/10.1016/j.conbuildmat.2016.10.035>
- [15] GARCIA FILHO, F.C., LUZ, F.S., OLIVEIRA, M.S., *et al.*, “Thermal behavior of graphene oxide-coated piassava fiber and their epoxy composites”, *Journal of Materials Research and Technology*, v. 9, n. 3, pp. 5343–5351, 2020. doi: <http://dx.doi.org/10.1016/j.jmrt.2020.03.060>
- [16] REBELO, V., SILVA, Y., FERREIRA, S., *et al.*, “Effects of mercerization in the Chemical and morphological properties of amazon piassava”, *Polímeros*, v. 29, n. 1, pp. 1–6, 2019. doi: <http://dx.doi.org/10.1590/0104-1428.01717>
- [17] SANTOS, E.B.C., MORENO, C.G., BARROS, J.J.P., *et al.*, “Effect of alkaline and hot water treatments on the structure and morphology of piassava fibers”, *Materials Research*, v. 21, n. 2, 2018. doi: <http://dx.doi.org/10.1590/1980-5373-mr-2017-0365>
- [18] MIRANDA, C.S., FIUZA, R.P., CARVALHO, R.F., *et al.*, “Efeito dos tratamentos superficiais nas propriedades do bagaço da fibra de piaçava *Attalea funifera Martius*”, *Química Nova*, v. 38, n. 2, pp. 161–165, 2015.
- [19] D’ALMEIDA, A.L.F.S., D’ALMEIDA, J.R.M., BARRETO, D.W., *et al.*, “Effect of surface treatments on the thermal behavior and tensile strength of piassava (*Attalea funifera*) fibers”, *Journal of Applied Polymer Science*, v. 120, n. 5, pp. 2508–2515, 2011. doi: <http://dx.doi.org/10.1002/app.33349>
- [20] JOSE, S., THOMAS, S., JIBIN, K.P., *et al.*, “Surface modification of wool fabric using sodium lignosulfonate and subsequent improvement in the interfacial adhesion of natural rubber latex in the wool/rubber composites”, *Industrial Crops and Products*, v. 177, pp. 114489, 2022. doi: <http://dx.doi.org/10.1016/j.indcrop.2021.114489>
- [21] OLIVEIRA, F., SILVA, C.G., RAMOS, L.A., *et al.*, “Phenolic and lignosulfonate-based matrices reinforced with untreated and lignosulfonate-treated sisal fibers”, *Industrial Crops and Products*, v. 96, pp. 30–41, 2017. doi: <http://dx.doi.org/10.1016/j.indcrop.2016.11.027>
- [22] GUALBERTO, S.L., MOTTA, L.A.C., PASQUINI, D., “Treatment of sisal fibers with lignosulphonate to improve the properties of fiber cement composites”, *Revista Virtual de Química*, v. 13, n. 6, pp. 1257–1267, 2021. doi: <http://dx.doi.org/10.21577/1984-6835.20210077>

- [23] LI, H., FU, S., PENG, L., *et al.*, “Surface modification of cellulose fibers with layer-by-layer self-assembly of lignosulfonate and polyelectrolyte: effects on fibers wetting properties and paper strength”, *Cellulose (London, England)*, v. 19, n. 2, pp. 533–546, 2012. doi: <http://dx.doi.org/10.1007/s10570-011-9639-3>
- [24] WANG, Q., WANG, J., LIANG, W., *et al.*, “Improved mechanical properties of jute fiber/polypropylene composite with interface modified by sodium lignosulfonate”, *Journal of Biobased Materials and Bioenergy*, v. 14, n. 2, pp. 186–194, 2020. doi: <http://dx.doi.org/10.1166/jbmb.2020.1957>
- [25] RUWOLDT, J., “A critical review of the physicochemical properties of lignosulfonates: chemical structure and behavior in aqueous solution, at surfaces and interfaces”, *Surfaces*, v. 3, n. 4, pp. 622–648, 2020. doi: <http://dx.doi.org/10.3390/surfaces3040042>
- [26] PARK, S., BAKER, J.O., HIMMEL, M.E., *et al.*, “Cellulose crystallinity index: measurement techniques and their impact on interpreting cellulase performance”, *Biotechnology for Biofuels*, v. 3, n. 1, pp. 10–19, 2010. doi: <http://dx.doi.org/10.1186/1754-6834-3-10>. PubMed PMID: 20497524.
- [27] SEGAL, L., CREELY, J.J., MARTIN JUNIOR, A.E., *et al.*, “An empirical method for estimating the degree of crystallinity of native cellulose using the X-Ray diffractometer”, *Textile Research Journal*, v. 29, n. 10, pp. 786–794, 1962. doi: <http://dx.doi.org/10.1177/004051755902901003>
- [28] AMERICAN SOCIETY FOR TESTING AND MATERIALS, *ASTM E2224-19 Standard guide for forensic analysis of fibers by infrared spectroscopy*, West Conshohocken, ASTM International, 2019.
- [29] AMERICAN SOCIETY FOR TESTING AND MATERIALS, *ASTM E2550-21 Standard Test Method for Thermal Stability by Thermogravimetry*, West Conshohocken, ASTM International, 2021.
- [30] AMERICAN SOCIETY FOR TESTING AND MATERIALS, *ASTM C1557-20 Standard Test Method for Tensile Strength and Young’s Modulus of Fibers*, West Conshohocken, ASTM International, 2020.
- [31] AMERICAN SOCIETY FOR TESTING AND MATERIALS, *ASTM E1756-08 (Reapproved 2015) Standard Test Method for Determination of Total Solids in Biomass*, West Conshohocken, ASTM International, 2015.
- [32] AMERICAN SOCIETY FOR TESTING AND MATERIALS, *ASTM E104-20a Standard Practice for Maintaining Constant Relative Humidity by Means of Aqueous Solutions*, West Conshohocken, ASTM International, 2020.
- [33] JAZI, M.E., NARAYANAN, G., AGHABOZORGI, F., *et al.*, “Structure, chemistry and physicochemistry of lignin for material functionalization”, *SN Applied Sciences*, v. 1, n. 9, pp. 1094–1112, 2019. doi: <http://dx.doi.org/10.1007/s42452-019-1126-8>
- [34] MACHMUDAH, S., DIONO, W., KANDA, H., *et al.*, “Hydrolysis of biopolymers in near-critical and subcritical water”, In: González, H.D., Muñoz, M.J.G. (eds.), *Water extraction of bioactive compounds*, chapter 3, Amsterdam, Elsevier, pp. 69–107, 2017.
- [35] OVALLE-SERRANO, A.S., BLANCO-TIRADO, C., COMBARIZA, M.Y., “Exploring the composition of raw and delignified Colombian fique fibers, tow and pulp”, *Cellulose (London, England)*, v. 25, n. 1, pp. 151–165, 2018. doi: <http://dx.doi.org/10.1007/s10570-017-1599-9>
- [36] FERREIRA, S.R., SILVA, F.A., LIMA, P.R.L., *et al.*, “Effect of fiber treatments on the sisal fiber properties and fiber-matrix bond in cement based systems”, *Construction & Building Materials*, v. 101, pp. 730–740, 2015. doi: <http://dx.doi.org/10.1016/j.conbuildmat.2015.10.120>
- [37] YANG, H., YAN, R., CHEN, H., *et al.*, “Characteristics of hemicellulose, cellulose and lignin pyrolysis”, *Fuel*, v. 86, n. 12–13, pp. 1781–1788, 2007. doi: <http://dx.doi.org/10.1016/j.fuel.2006.12.013>
- [38] MONTEIRO, S.N., LOPES, F.P.D., FERREIRA, A.S., *et al.*, “Natural-fiber polymer-matrix composites: cheaper, tougher, and environmentally friendly”, *JOM*, v. 61, n. 1, pp. 17–22, 2009. doi: <http://dx.doi.org/10.1007/s11837-009-0004-z>
- [39] BASU, P., “Torrefaction”, In: BASU, P. (ed.), *Biomass gasification, pyrolysis and torrefaction*, chapter 4, Cambridge (MA), Academic Press, pp. 87–145, 2013. doi: <http://dx.doi.org/10.1016/B978-0-12-396488-5.00004-6>